Frequency Switching with the Arecibo Telescope

S. Stanimirovic & C. Salter (Arecibo Observatory)

June 3, 2002

1 Introduction

The technique of Frequency Switching (FS) is often used in spectral line observations. It consists of switching repeatedly between two phases: typically, (a) an observation at the central frequency ν, often called the 'Signal', followed by (b) an observation of the same celestial position centered at frequency $\nu + \Delta\nu$, often called the 'Reference' (see Fig. 1). The Signal and Reference spectra are observed sequentially at switching rates which give a shorter cycle time than changes in the hardware and environment. Combining Signal and Reference phases into a (Signal$-$Reference) spectrum, (as in the bottom half of Fig. 1), results in partial cancellation of the passband shape. The true sky distribution can then be extracted from the (Signal$-$Reference) spectrum in two ways: (1) by inverting and shifting the Reference spectrum by the known frequency interval, then subtracting Reference from Signal, and dividing by factor of 2; or (2) by convolution (see below). The former is only useful if the total line width of the feature of interest is less than the magnitude of the frequency switch.

The main purpose of the FS technique is to provide flat baselines without observing a nearby emission-free region, as in Position Switching. Indeed, for FS, both Signal and Reference spectra are obtained 'on-source'. For very extended sources, (e.g. Galactic HI, Magellanic Stream, high velocity clouds), that are much larger than the telescope beam, frequency switching gives better results than position switching as it is often hard, or even impossible, to find an nearby emission-free region that would properly represent the passband.

One of the biggest obstacles for implementing the FS technique for the Arecibo telescope are spectral standing waves. These occur because broad-band signals (e.g. the Sun, RFI, Galactic HI, strong radio continuum sources, ground radiation, etc.) may enter the receiving system via two or more paths of different lengths causing mutual interference. Although at many telescopes standing waves are dominated by a single periodicity, the extensive Arecibo feed support structure post-upgrade is situated in the ray path of the incoming radiation, and produces complex standing-wave patterns due to multiple wave scattering. This has led to the FS technique not being employed at Arecibo post-upgrade, as even shifts as small as 1 MHz or less (equivalent to $\Delta v_r \approx 210$ km s^{-1} at 1420 MHz) can fail to cancel the standing wave pattern in the (Signal$-$Reference) spectrum, leaving

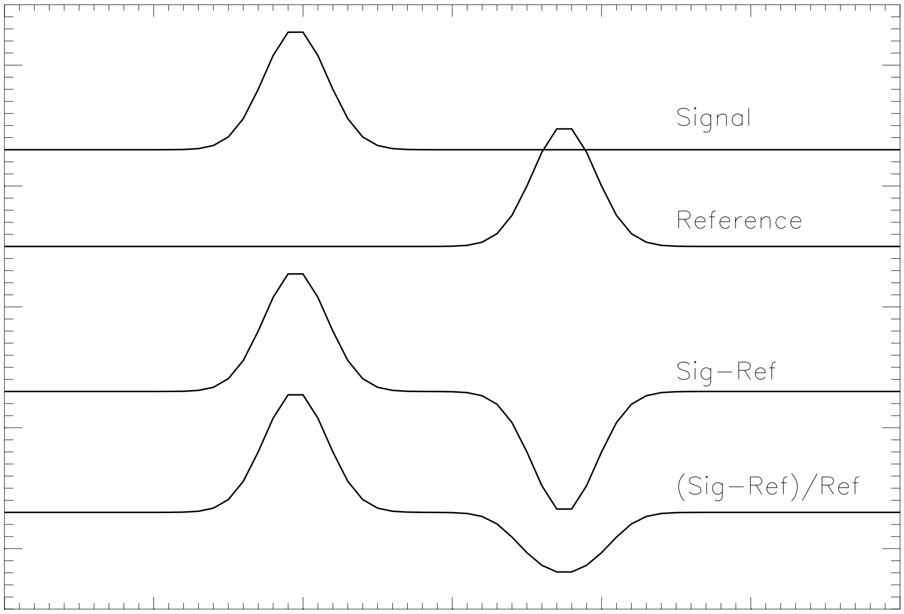

Figure 1: A schematic diagram of frequency switched observations. Signal and Reference spectra are obtained by a shift of $\Delta\nu$ in the central frequency. (Signal−Reference) or (Signal−Reference)/Reference spectra are shown in the lower half of the figure. The (Signal−Reference) spectrum preserves the amplitudes of the line features.

baselines of poor quality. For a more detailed consideration, see Appendix A.

Briggs et al. (1997) investigated spectral standing waves at Arecibo from the data taken for a drift-scan survey with the pre-upgrade L-band line feed and showed that it is possible to characterize complex standing wave patterns for this particular observing mode and successfully remove them from the data. They showed that these waves vary in amplitude and phase; this results in their successful subtraction when a simple passband calibration is applied. Salter & Ghosh (http://www.naic.edu/~astro/atoms/performance.shtml, and there click on 2001-02.ps) have given examples of the standing waves generated by a point source in the main beam observed from the Gregorian dome with the L-band Wide receiver.

Driven by the wide use that the FS technique could have for mapping Galactic HI, we have recently undertaken several observational tests in order to explore and try possible solutions that may enable FS to be used at Arecibo.

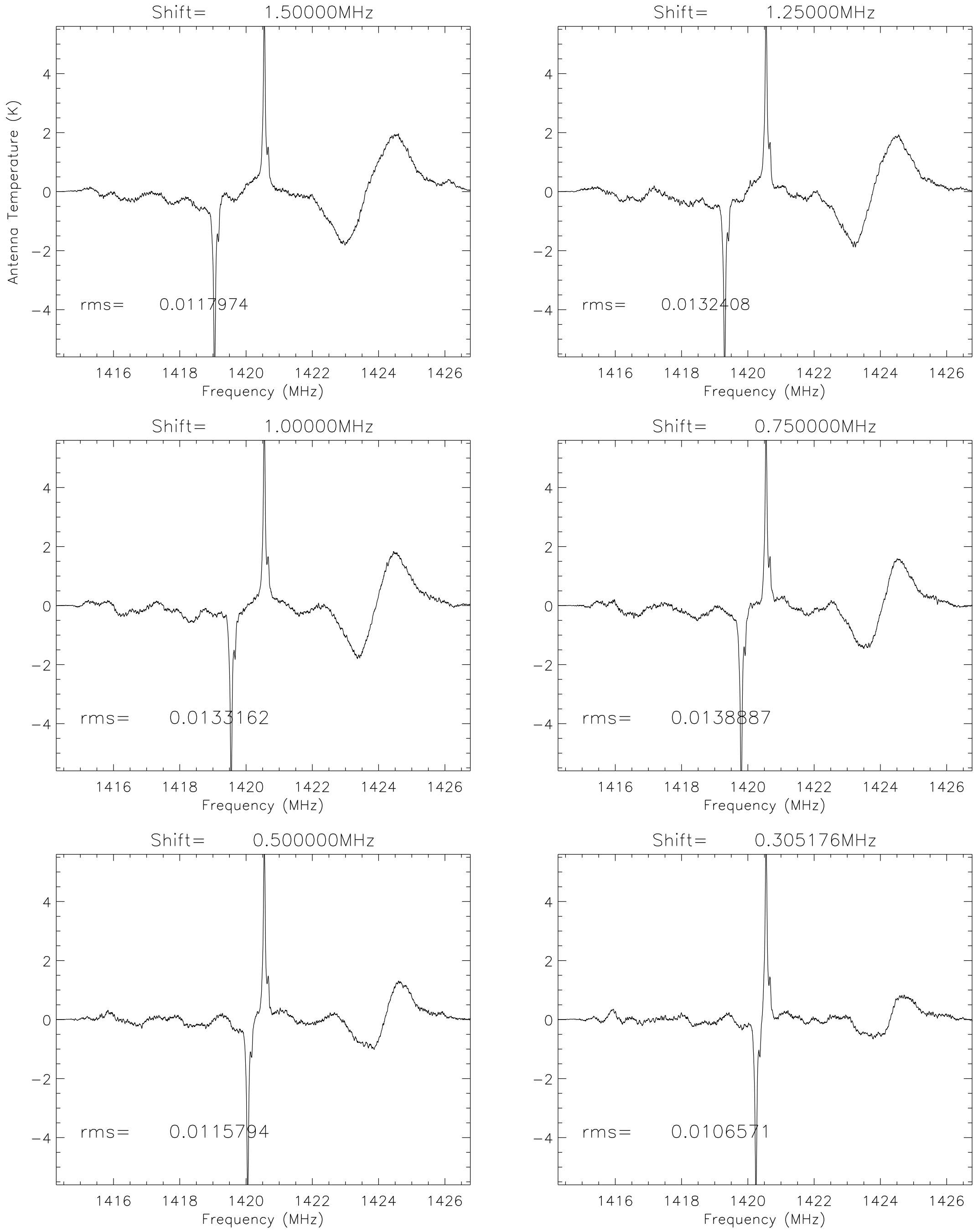

Figure 2: Frequency-switched observations with the L-band Wide receiver. The bandwidth is 12.5 MHz divided into 2048 spectral channels. (Signal−Reference) spectra are shown, where the frequency shift was varied from 1.5 to 0.076 MHz. The broad feature around 1424.3 MHz is a trapped-mode resonance in the receiver feed. The rms noise was measured over frequency range 1415.5 – 1418 MHz.

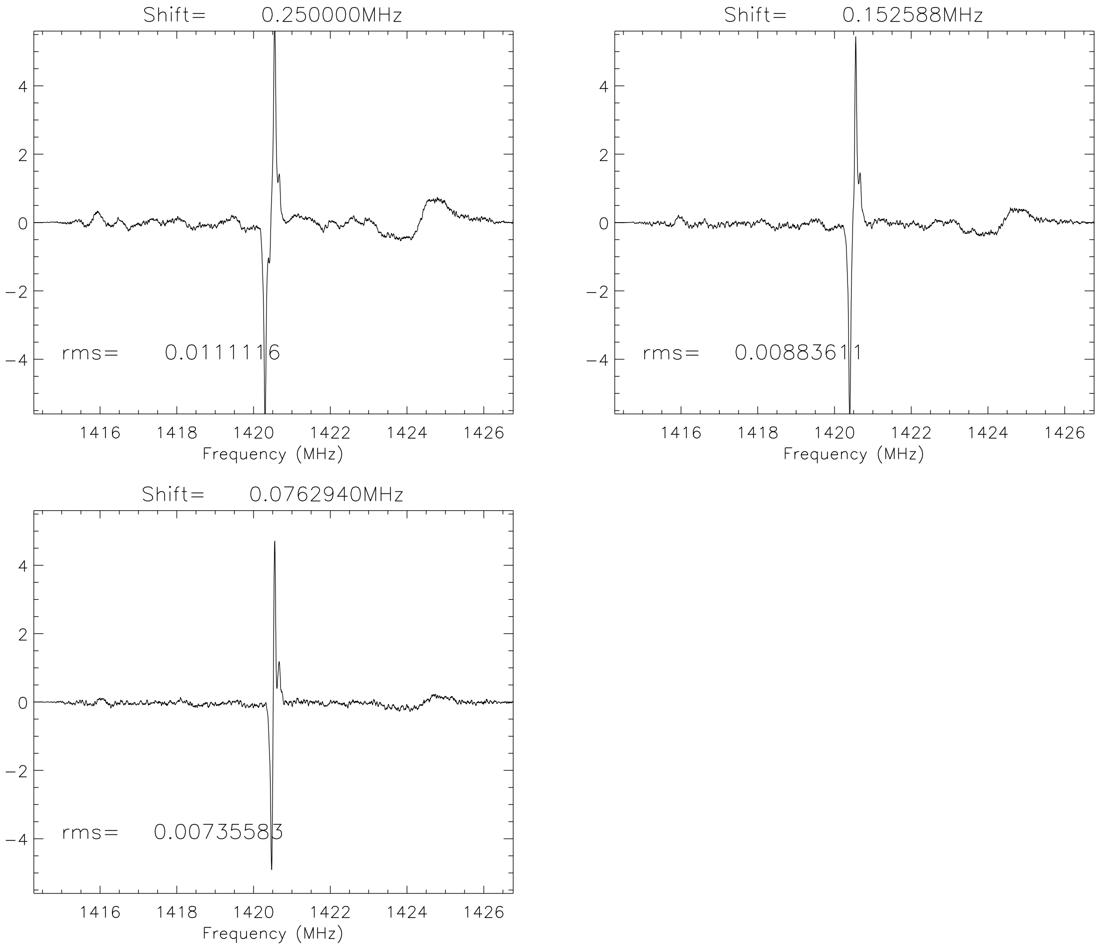

Figure 2: *continued*

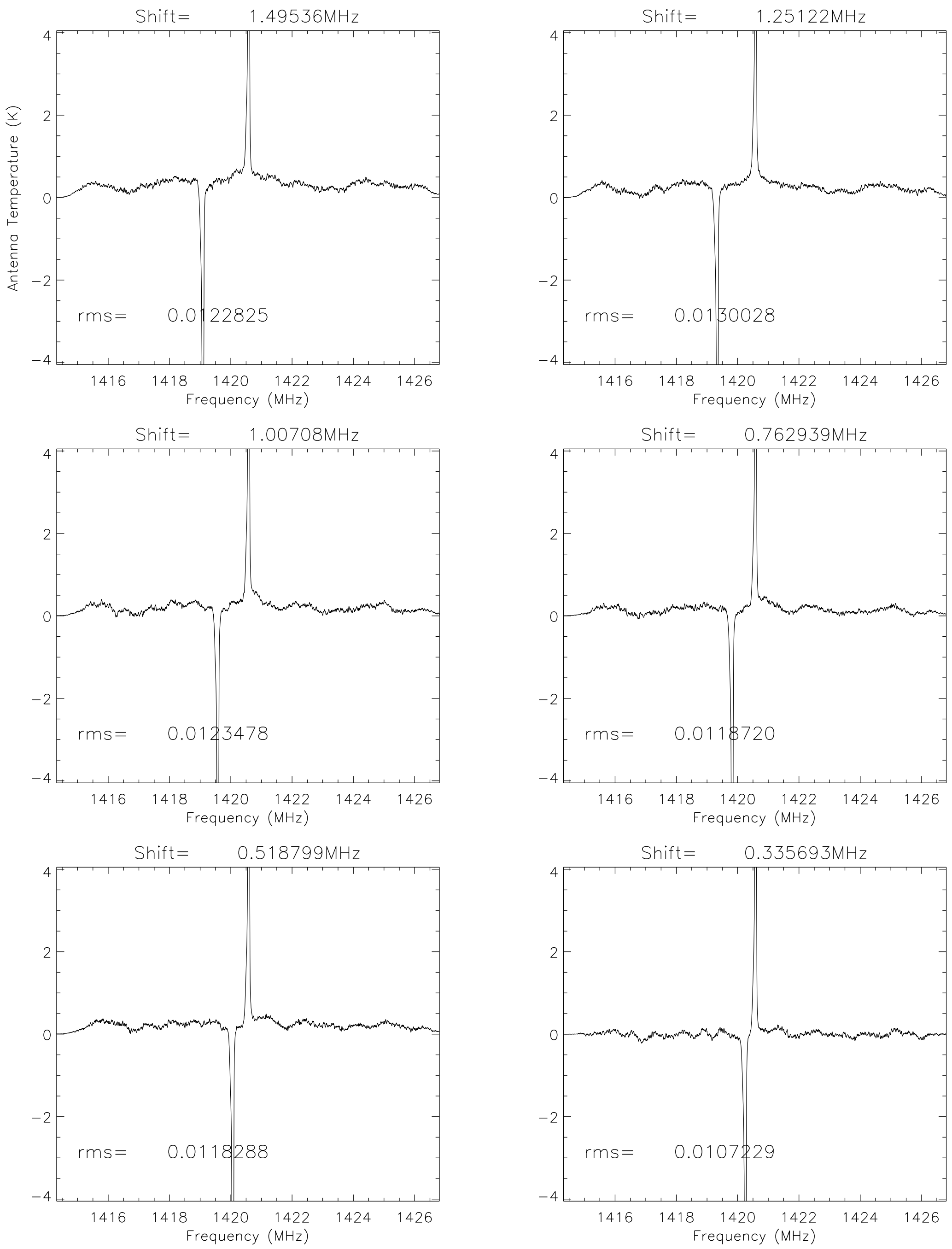

Figure 3: Frequency-switched observations with the L-band narrow receiver. The bandwidth is 12.5 MHz divided into 2048 spectral channels. (Signal−Reference) spectra are shown, where the frequency shift was varied from 1.5 to 0.018 MHz. The rms noise was measured over frequency range 1415.5 – 1418 MHz.

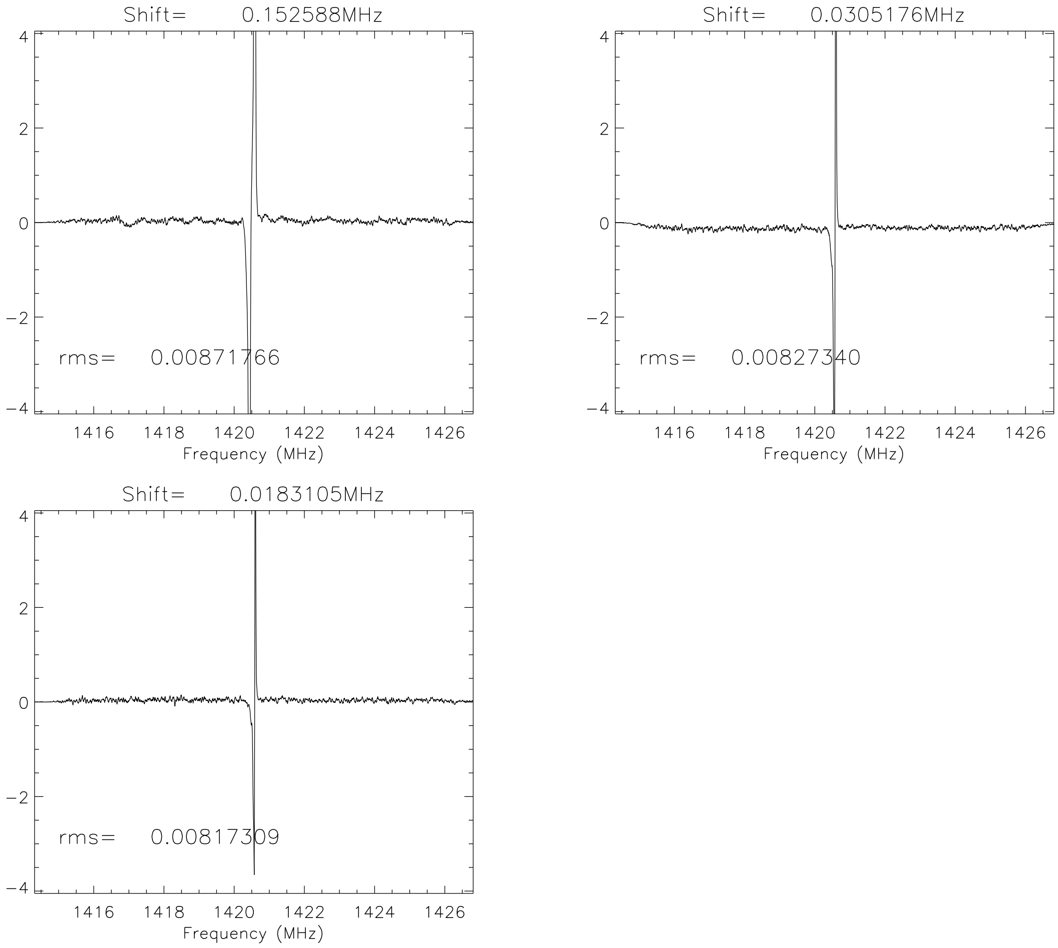

Figure 3: *continued*

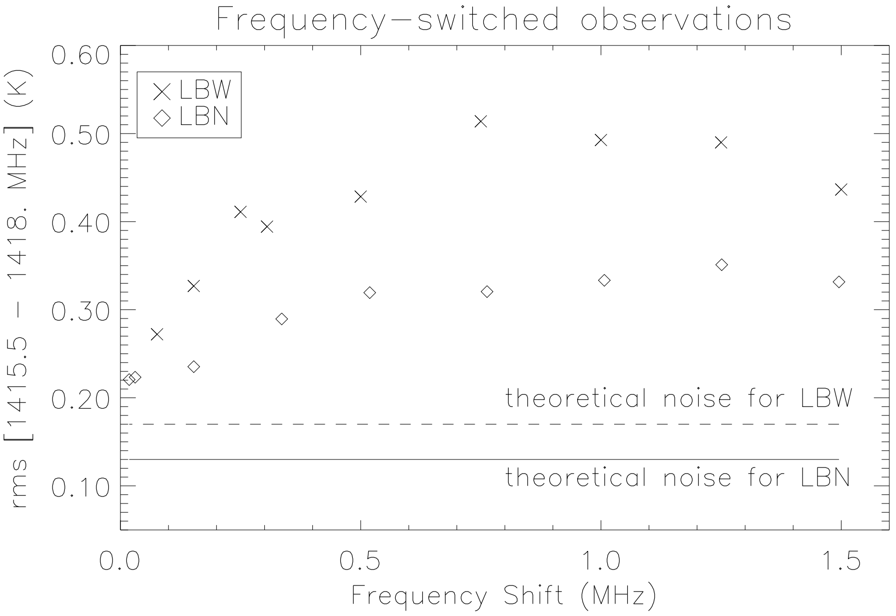

Figure 4: The rms noise in (Signal−Reference) spectra as a function of the frequency switching step. The LBN data are shown by diamonds and the LBW data by crosses. Theoretical estimates were obtained for an observational bandwidth of 12.5 MHz, 2048 channels, 10 sec of integration per data dump and 3 pairs of switched spectra.

2 Observational Tests of Frequency Switching

We have obtained frequency-switched observations towards several Galactic positions while varying the frequency switching step $\Delta\nu$ from 1.5 to 0.07 MHz. Figure 2 shows the data obtained with the L-band wide (LBW) receiver, while Figure 3 gives data obtained with the L-band narrow (LBN) receiver. For both figures, (Signal−Reference) spectra are presented. The spectra show considerable residual baseline fluctuations, especially when $\Delta\nu > 0.15$ MHz. Most of these features are likely to be due to standing-wave contributions that did not cancel fully. Note that there is no quasi-sinusoidal periodicity that would be easy to remove. In addition, the LBW receiver has worse baseline ripples than does LBN. The large 'S'-shaped feature around 1424.3 MHz (Fig. 2) corresponds to a known trapped-mode resonance for this receiver. For $\Delta\nu < 0.15$ MHz, the resultant baselines are significantly flatter. However, for these cases the broad HI emission lines present in the Signal and Reference spectra overlap, resulting in mutual confusion in the final spectrum. The true signal buried in the difference spectrum cannot now be simply extracted and requires more sophisticated treatment.

Fig. 4 compares the rms noise in the (Signal−Reference) spectra for both receivers as measured on a range of signal-free channels as a function of the frequency shift ($\Delta\nu$). The theoretically-expected noise levels are also shown. For both receivers, the noise significantly increases with the magnitude of the switching step, with this rise being steeper for the LBW receiver. In both cases, for the smallest switching steps the estimated noise is within factor of 2 of the theoretically-predicted values.

For both the LBN and LBW receivers, frequency switching of smaller magnitude ($\lesssim$ 0.3 MHz) provides much flatter baselines than switching by larger amounts. However, the problem then becomes line reconstruction as Signal and Reference lines overlap and blend together.

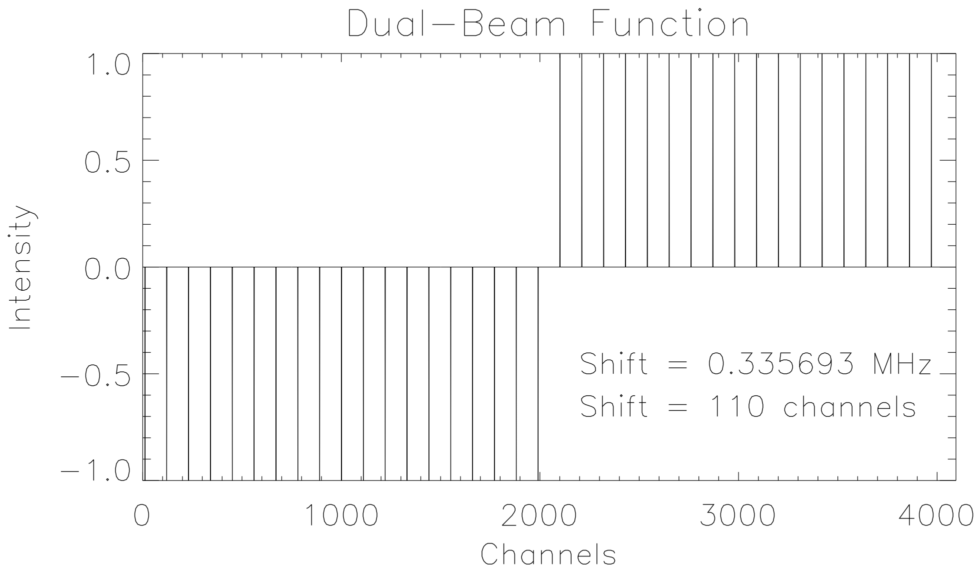

Figure 5: The 'dual-beam' function used for convolution with the frequency switched signal in the Emerson et al. (1979) algorithm. The size (number of elements in an one-dimensional array) of this function is twice the size of the observed spectrum. The difference between each two adjacent delta-functions is equal to the frequency switching step, $\Delta\nu$.

3 Reconstruction Algorithm

The reconstruction algorithm of Emerson et al. (1979) was devised to handle dual-beam radio-continuum mapping of spatially extended objects using a telescope beam throw smaller than the size of the object. Frequency switching is effectively equivalent to the dual-beam scanning case, in which beam switching is used to cancel the effects on the scan baseline of fluctuations due to the atmospheric emission. For observing objects whose angular sizes are smaller than the magnitude of the beam switch a "shift and subtract" analysis can be employed. When the source angular size is comparable to, or greater than, the separation between the two beams, the problem of image reconstruction is the same as for frequency switching by an amount smaller than the line width. Indeed, Emerson et al. (1979) suggested that their technique would be appropriate for application to FS spectral-line observations. The technique was "rediscovered" and applied by Liszt (1997) in order to process FS data obtained with a switching interval that was smaller than the extent of the signal-bearing region.

The fundamental conclusion of Emerson et al. and Liszt was that the true spectral distribution can be recovered from the FS records by convolving the (Signal−Reference) spectra with a simple comb function as shown in Fig. 5. We will refer to this convolving function as the dual-beam function. In this way, the true spectral distribution is fully recovered, hopefully with an improved passband. In order to minimize the noise level resulting from the reconstruction process, only the signal-bearing part of the (Signal−Reference) spectrum should be used. The algorithm can recover both narrow and broad spectral lines. One effect of application of this algorithm is that the final noise is a function of "spatial frequency" within the spectrum. The signal-to-noise ratio post-reconstruction degrades rapidly for structure whose total extent is $\gtrsim 4 \times \Delta\nu$.

4 Results of Spectral Reconstruction

As an example of how the reconstruction algorithms works in practice we show its application on the FS data for a broad Galactic HI line (~ 100 km s^{-1} wide). Bandwidth of 6.25 MHz was used over 2048 correlator channels. Three pairs of (Signal, Reference) spectra, each observed for 10 sec, were obtained. Signal-Reference spectra were derived for each polarization and averaged. Results from each of three (Signal, Reference) pairs were also averaged. The next step was to fit and subtract a linear polynomial function to remove a very large scale gradient if present. An emission-free range of channels, 200 – 500 and 1300 – 1800, was used for this purpose. The signal-bearing part of the resultant spectrum, corresponding to the channel range 640 – 1240, was then convolved with the dual-beam function shown in Fig. 5. The final spectrum was divided by 2. This spectrum is shown in the bottom panel of Fig. 6. For comparison, only Signal spectrum is shown in the middle panel. The reconstructed spectrum reproduces remarkably well multiple line features seen in the Signal only spectrum. In addition it has a flat, featureless baseline, whose rms noise is comparable to that of the Signal spectrum.

Another example of an HI line is shown in Fig. 7 for a slightly narrower line, ~ 50 km s^{-1} wide. A very small frequency switching step of 0.07 MHz was used here.

4.1 Finding the Optimum Switching step

In order to investigate whether there is an optimum switching step for the data presented above, we have produced reconstructed spectra for the strong, broad HI spectrum shown in Fig. 6 for various frequency switching steps ($\Delta\nu$), starting with 1.5 MHz down to 0.018 MHz, (see Fig. 8). **The profile for all these spectra are very well reproduced.** However, the noise is obviously

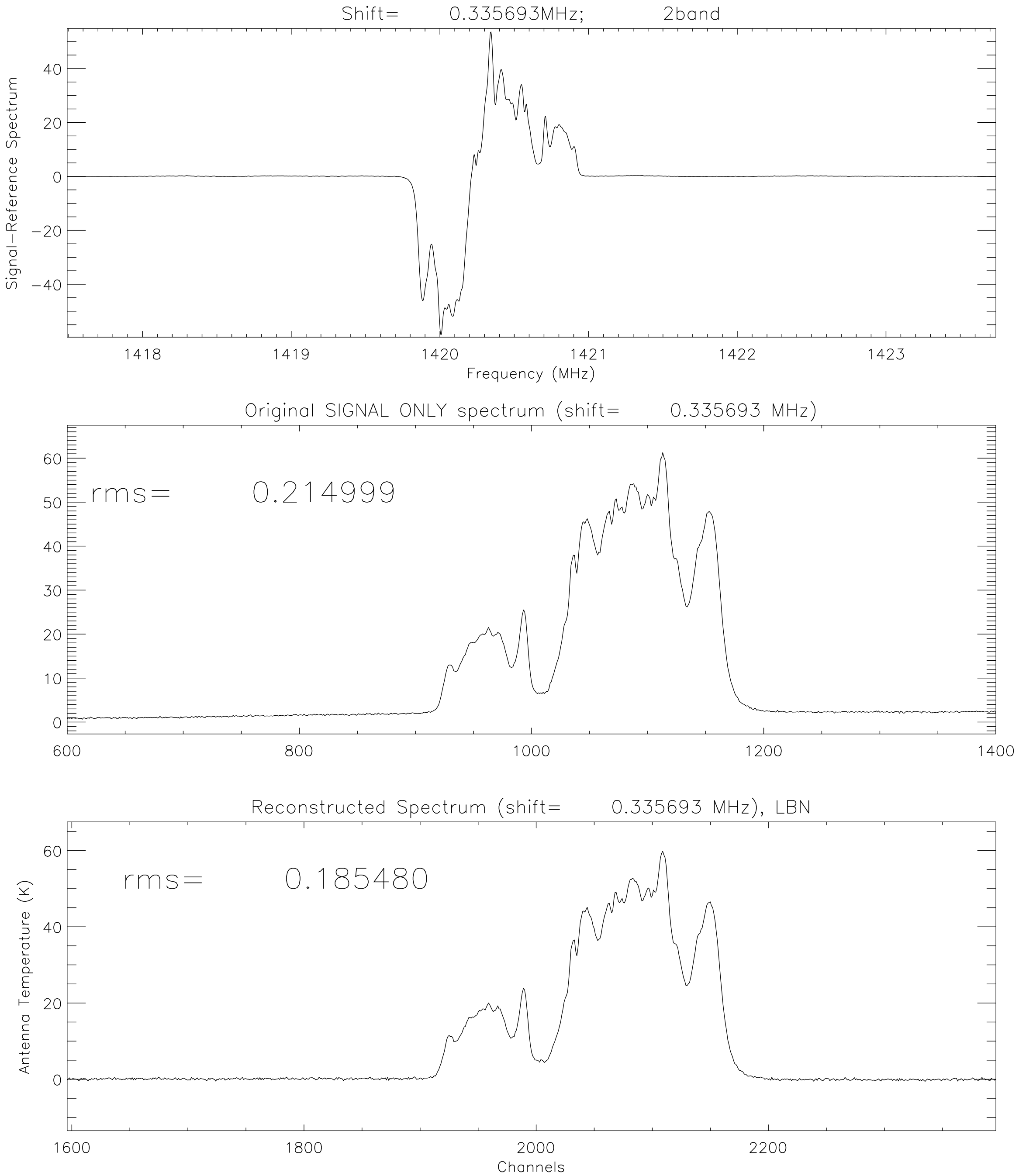

Figure 6: (top panel) The (Signal−Reference) spectrum. (middle panel) The Signal-only spectrum with a mean value over the channel range 200 – 500 having been subtracted. The rms noise was measured over the channel range 650 – 800. (bottom panel) The reconstructed spectrum. The rms noise was measured over the channel range 1650 – 1800. Observations were obtained with the LBN receiver.

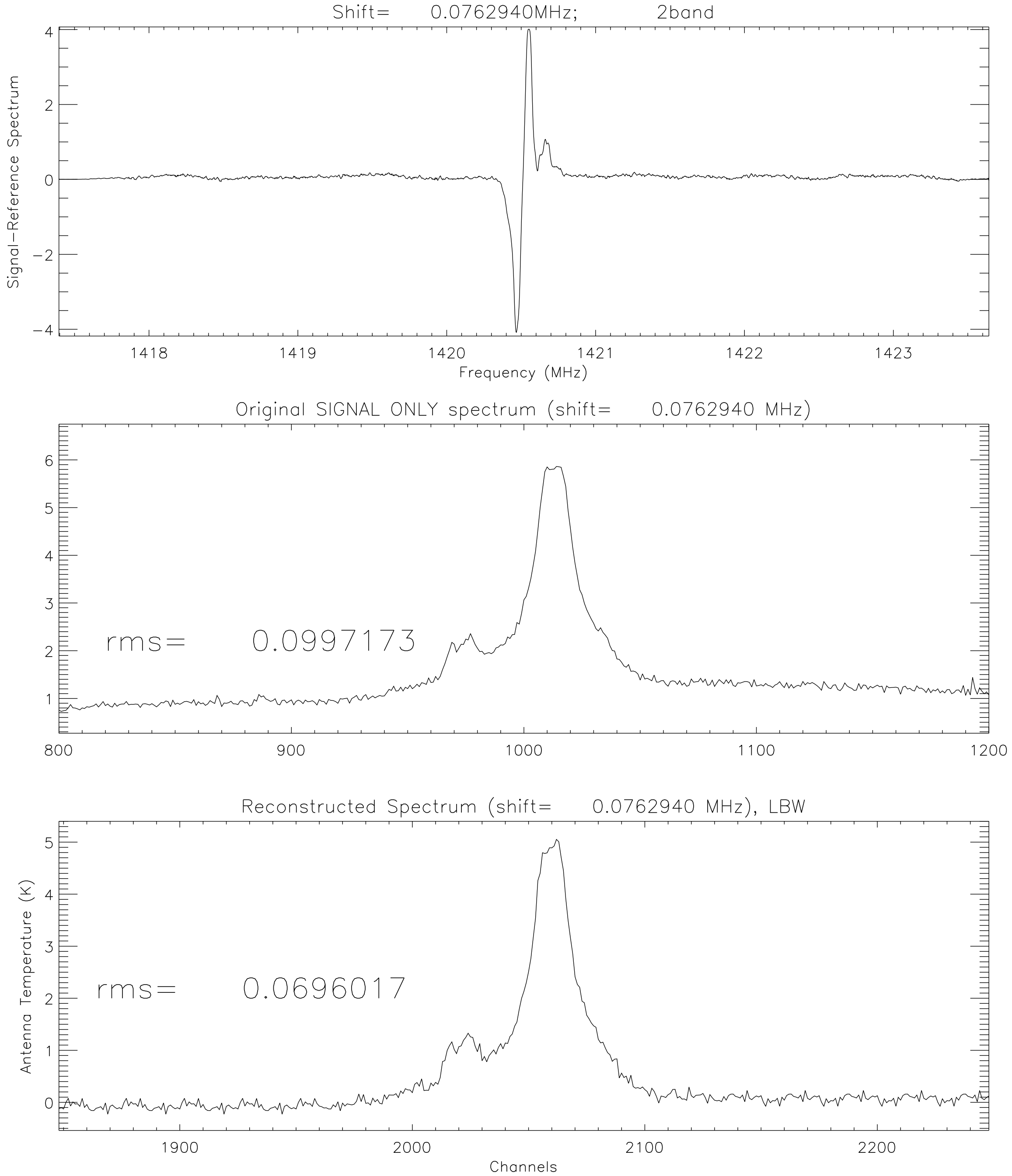

Figure 7: As in Figure 6. Observations were obtained with the LBW receiver.

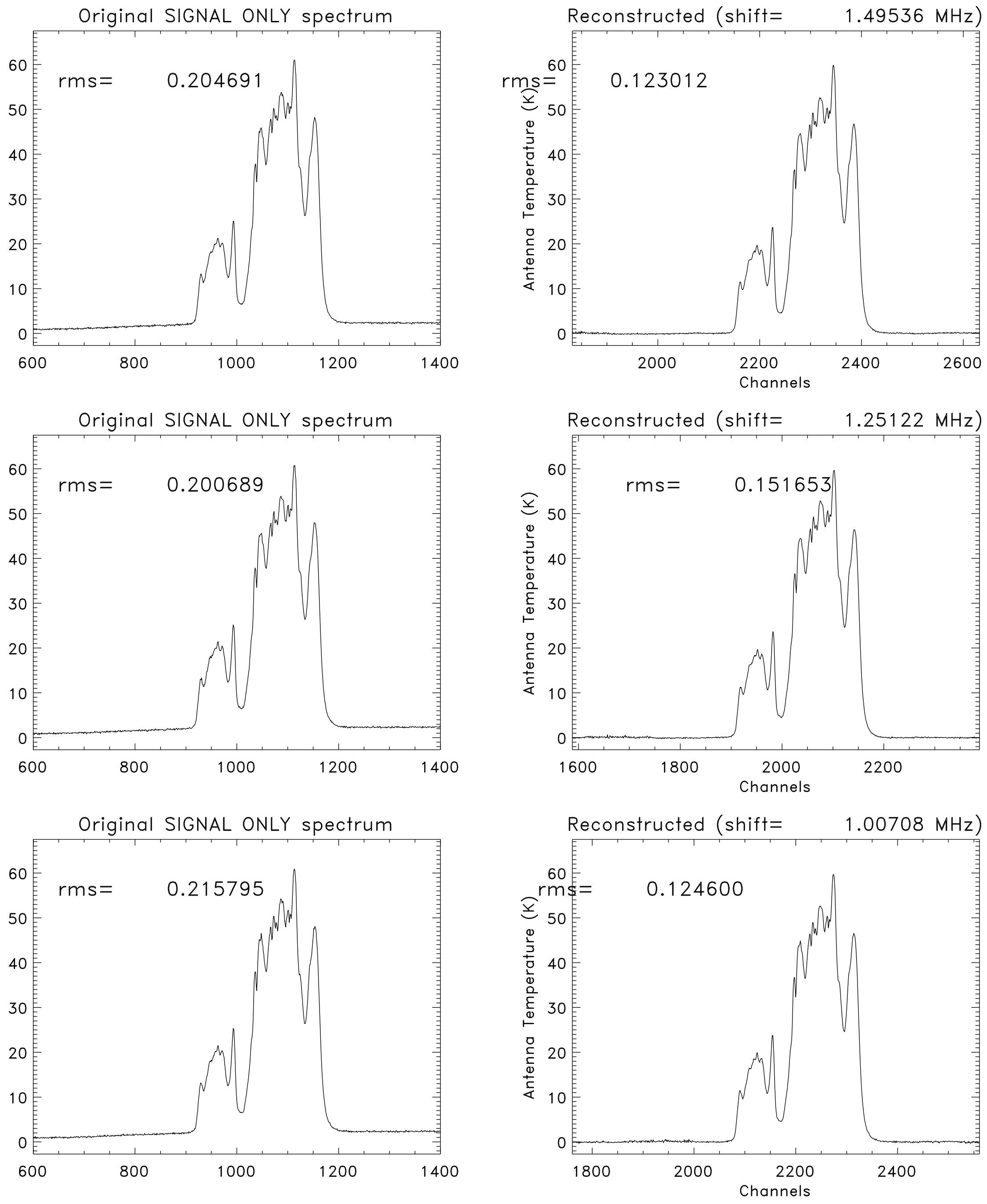

Figure 8: The reconstructed broad HI spectrum for various frequency-switching steps, $\Delta\nu$. The left-hand plots show the Signal-only spectra, while the reconstructed spectra are displayed on the right-hand plots.

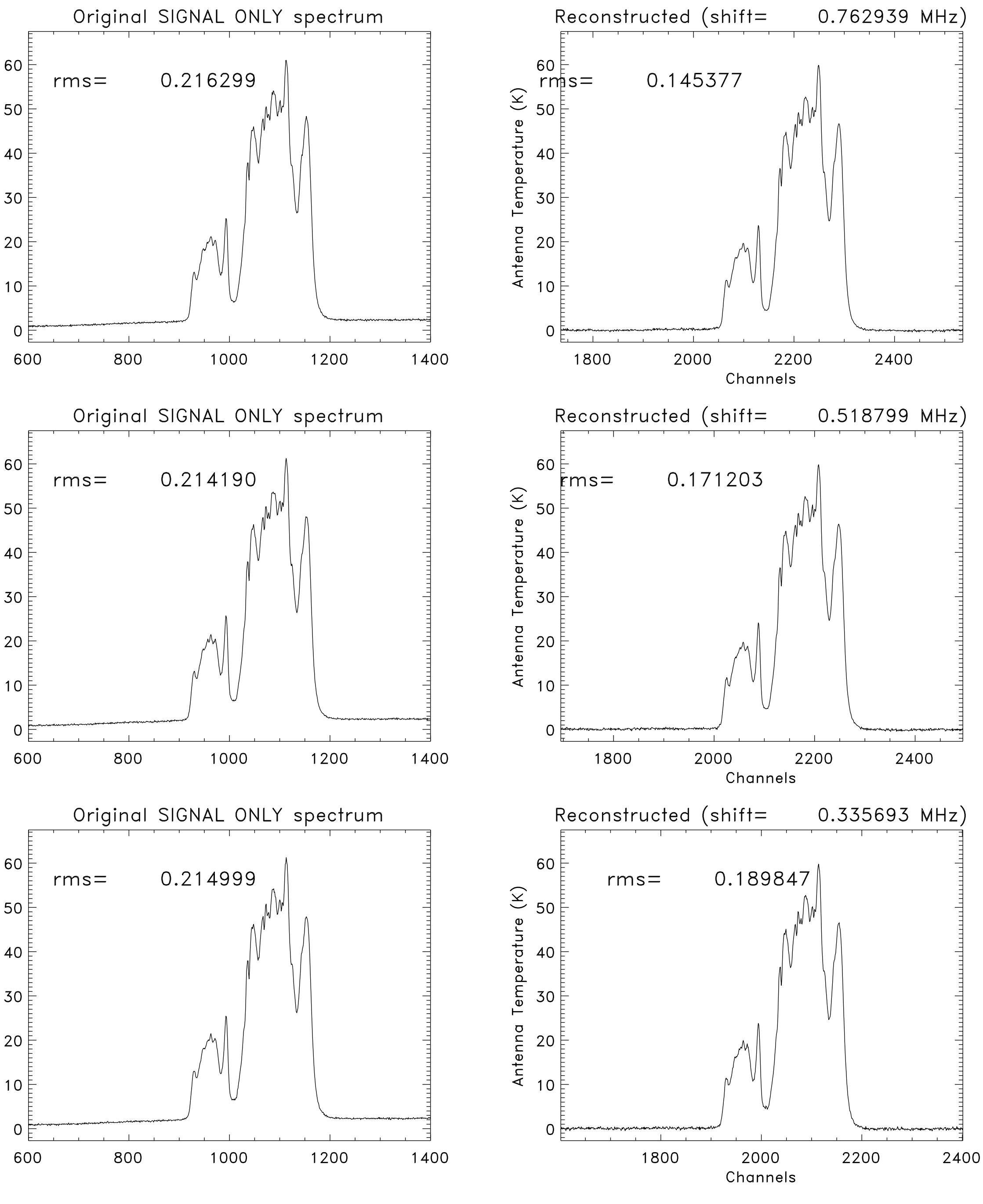

Figure 8: *continued*

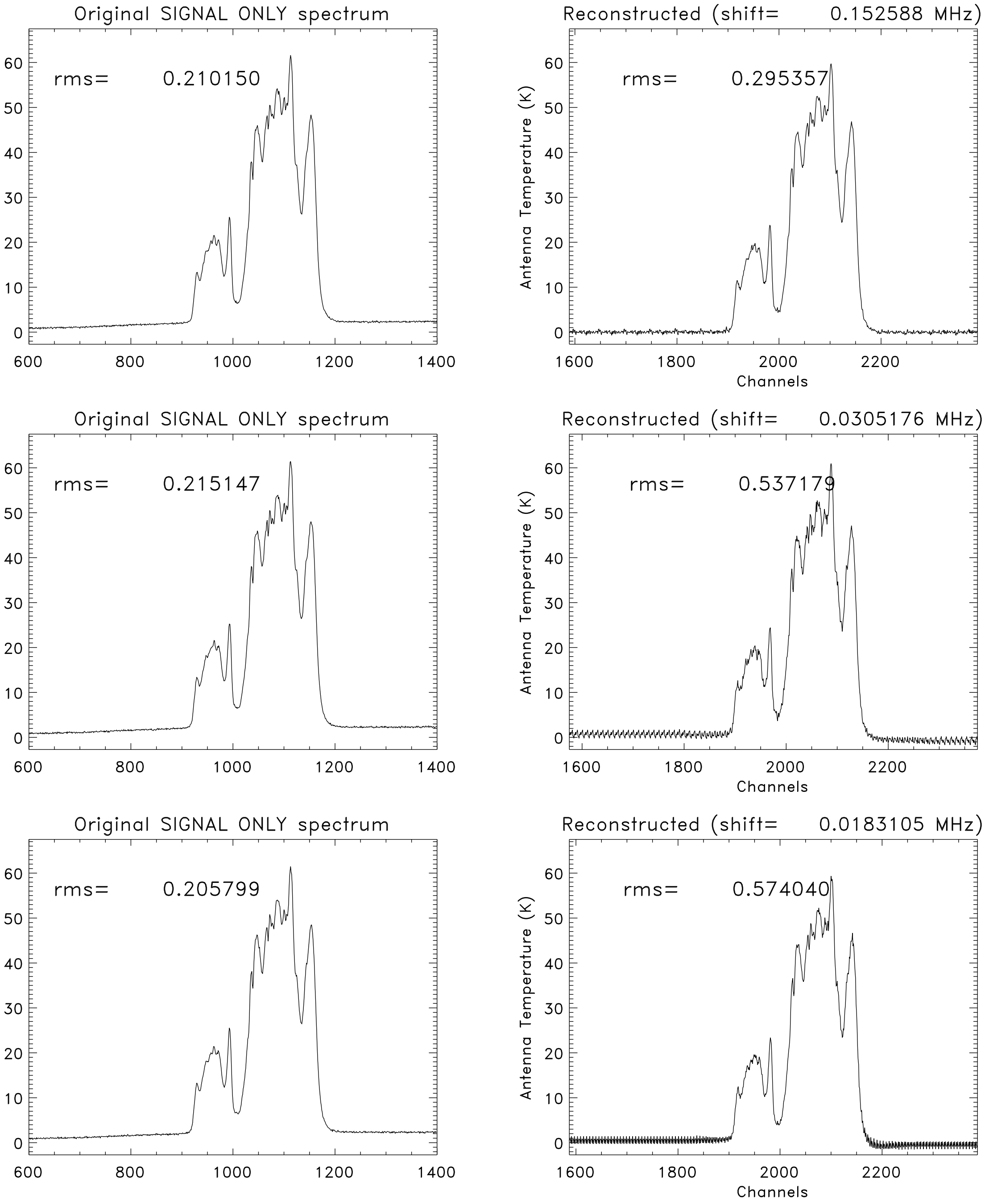

Figure 8: *continued*

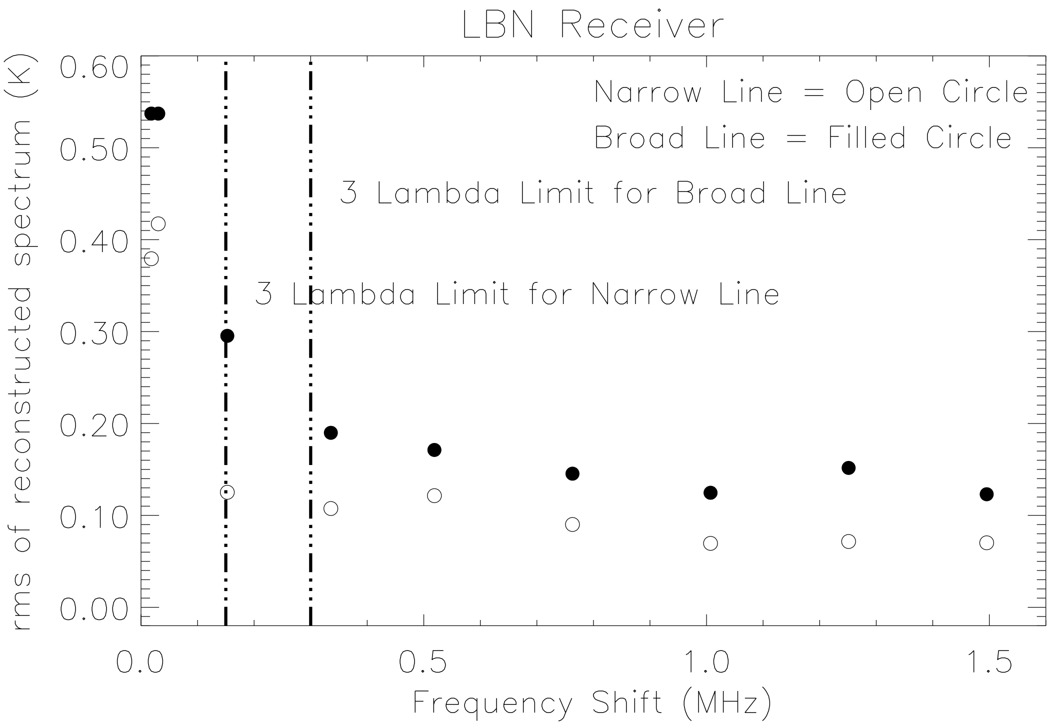

Figure 9: The rms noises in the reconstructed spectra as a function of the frequency switching step, $\Delta\nu$. Filled circles represent the broad HI line from Fig. 6 ,while the open circles correspond to the narrower HI line from Fig. 7. The theoretical noise level is $\approx$0.13 K. The $3 \times \lambda$ limits represent switching steps below which a significant increase in the noise should be noticeable.

higher for $\Delta\nu = 0.030$ and 0.018 MHz. The rms noises in the reconstructed spectra are plotted in Fig. 9 as a function of $\Delta\nu$. In this figure, results for both the spectral lines of Figs. 6 and 7 are presented.

Emerson et al. (1979) showed that the reconstructed spectra should have superior noise for the cases when the emission-bearing region is $\leq (3-4) \times \Delta\nu$. This sets an lower limit for $\Delta\nu$ relative to the extent of the observed line. We thus present the $3 \times \lambda$ limits on the frequency-switching step as vertical dot-dashed lines in Fig. 9 . If the frequency steps are smaller than these limits the rms noise in the reconstructed spectra should start to deteriorate, exactly in agreement with we find for our data. Especially for the broad lines, the rms noise flattens around $\Delta\nu = 0.5 - 1$ MHz. For $\Delta\nu > 0.5$ MHz we would expect noise to "saturate" or even to start increasing again due to the telescope standing waves. No increase is obvious from the data, doubtless because both of these lines are very strong, so that we have not here reached the level where standing waves dominate.

5 Future Work

To be done:

1. **Compare freq. switched with position switched data for the same source (to be reduced and compared).**

2. **Incorporate the use of non-integer number of channels for shifts.**

3. **To investigate calibration schemes, such as that leading to equation 6 in Appendix A.**

4. **To observe weak, broad lines to investigate the range of usefulness of frequency switching at Arecibo in terms of depth of integration possible, dependence on line width, etc. We note that the "beam-switching" application of the Emerson et al. algorithm, for which it was initially devised, aims to remove the effects of atmospheric emission. This contributes to the signal received by each beam essentially equally, and can be subtracted out to high accuracy provided the beam separation is not too wide, or the switching rate too slow. The frequency switching analog might be thought of as a broad-band, time variable passband variation. Frequency switching at Arecibo have a somewhat different problem to deal with in the form of standing waves that may vary only slowly as the telescope tracks a source, and trapped-mode resonances that are essentially time invariant. Both of these have similar frequency scales to the HI lines from galactic and extragalactic sources. However, while the quality of frequency switching should improve with decreasing line width, it is important to compare this observing mode with "pure total-power" observations.**

5. **When available, to experiment with the effects on the standing-wave pattern of moving the tertiary. This could help mitigate standing waves caused by derect reflections between the feed and the vertex of the dish.**

Appendix

A: A More Detailed Consideration of Frequency Switching

To describe the measurement process for a frequency-switched, spectral-line observation, we refer the system temperature to the the point at which the noise diode signal is injected. Let $T_{rx}(\nu)$ be the receiver noise temperature, $T_{source}(\nu)$ the antenna temperature of the target radio source and $T_{2.7K}$ that of the Cosmic Microwave Background (both in the absence of baseline ripples). Further, let $T_{spill}(\nu)$ be the contribution of all distributed emission received from outside the main beam (e.g. spillover from the ground, atmospheric emission, galactic background radiation, etc.) *including* the effects of the net baseline ripple applicable to this component. In addition, let g_{rf} be the receiver gain from calibration coupler to the mixer, and g_{be} the gain from the mixer to data recording, and g_{mb} be the frequency response of the telescope itself from aperture plane to calibration coupler for celestial radiation received in the telescope main beam (including the associated baseline ripples from standing waves). Suppose that the frequency switching is at the first mixer, and is between center frequency settings of $\nu_0 - \Delta\nu/2$ (SIGnal phase) and $\nu_0 + \Delta\nu/2$ (REFerence phase). Then, the signal recorded (referred to the calibration coupler) for the SIG phase of a frequency-switched observation is;

$$\mathrm{SIG}(\nu) = [\mathrm{T_{rx}}(\nu + \Delta\nu/2) + \mathrm{T_{source}}(\nu + \Delta\nu/2)\ \mathrm{g_{mb}}(\nu + \Delta\nu/2) + \mathrm{T_{2.7\,K}}\ \mathrm{g_{mb}}(\nu + \Delta\nu/2) + \mathrm{T_{spill}}(\nu + \Delta\nu/2)] * \mathrm{g_{rf}}(\nu + \Delta\nu/2) * \mathrm{g_{be}}(\nu) \quad (1)$$

The signal recorded for the REF phase is then;

$$\mathrm{REF}(\nu) = [\mathrm{T_{rx}}(\nu - \Delta\nu/2) + \mathrm{T_{source}}(\nu - \Delta\nu/2)\ \mathrm{g_{mb}}(\nu - \Delta\nu/2) + \mathrm{T_{2.7\,K}}\ \mathrm{g_{mb}}(\nu - \Delta\nu/2) + \mathrm{T_{spill}}(\nu - \Delta\nu/2)] * \mathrm{g_{rf}}(\nu - \Delta\nu/2) * \mathrm{g_{be}}(\nu) \quad (2)$$

Thus, if the data for the ON and OFF phases are subtracted,

$$\mathrm{SIG} - \mathrm{REF}(\nu) = \{\Delta[\mathrm{T_{rx}} * \mathrm{g_{rf}}](\nu, \Delta\nu) + \Delta[\mathrm{T_{source}} * \mathrm{g_{mb}} * \mathrm{g_{rf}}](\nu, \Delta\nu) + \Delta[\mathrm{T_{2.7\,K}} * \mathrm{g_{mb}} * \mathrm{g_{rf}}](\nu, \Delta\nu) + \Delta[\mathrm{T_{spill}} * \mathrm{g_{rf}}](\nu, \Delta\nu)\} * \mathrm{g_{be}}(\nu) \quad (3)$$

where $\Delta[\mathrm{x}](\nu, \Delta\nu) = [\mathrm{x}](\nu + \Delta\nu/2) - [\mathrm{x}](\nu - \Delta\nu/2)$. It is to be noted that if x varies only slowly with ν, then $\Delta[\mathrm{x}] \approx \mathrm{dx/dy}(\nu) * \Delta\nu$, i.e. if $\Delta\nu$ is much smaller than the frequency scale of all terms in eqn 1, then (SIG - REF) will approximate to the derivative of the total power. The situation usually encountered at telescopes where frequency switching is employed is that, (with the exception of the spectral line of interest which is confined to a spectral region that is smaller than $\Delta\nu$), the frequency scale of the terms in eqn 1, are indeed very much greater than $\Delta\nu$. Thus all terms in eqn 3 tend to zero, except for the line of interest, and two opposite-sign images of the spectral line are obtained, separated by $\Delta\nu$ and mutually non-overlapping.

At Arecibo, there are complications to this that result in a more complex situation than that just described. Firstly, the immense radius of curvature of the 305-m telescope results in standing-wave patterns that for a "single bounce" between the feed and the telescope vertex has a "wavelength" of very close to 1 MHz. However, the resultant standing-wave pattern is not a simple sinusoid (see http://www.naic.edu/~astro/atoms/performance.shtml, and there click on 2001-02.ps), but has a more complex form due to the many possible paths by which scattered radiation can be reflected to the feed (Briggs et al. 1997). In addition, trapped-mode resonances in the feed system (upstream of the calibration coupler) give narrow-band (of order 1 MHz again) contributions to $\Delta T_{rx}(\nu)$. Thus frequency switching by the step needed to produce non-overlapping galactic/extragalactic HI lines ($\gtrsim$ 1 MHz), are not expected to mitigate satisfactorily the contributions from these two sources of narrow-band variation.

We note that the situation described by eqn 3 can probably be improved somewhat (though not such as to mitigate the effects just described), by careful calibration. Supposing that the noise signal injected at the calibration coupler is pure white noise, (i.e. has no frequency dependence, and an equivalent power of T_{cal}), then an ON/OFF calibration measurement made for both of the frequency-switched settings can be used to eliminate some terms in eqn 3. The calibration "noise step", ΔCAL (i.e. $CAL_{ON} - CAL_{OFF}$) as recorded for the SIG frequency-switching phase is;

$$\Delta CAL^{SIG}(\nu) = T_{cal} * g_{rf}(\nu + \Delta\nu/2) * g_{be}(\nu) \tag{4}$$

and similarly, the calibration "noise step" as recorded for the REF frequency-switching phase is;

$$\Delta CAL^{REF}(\nu) = T_{cal} * g_{rf}(\nu - \Delta\nu/2) * g_{be}(\nu) \tag{5}$$

Hence, applying these measurements to bandpass correct (from the calibration coupler to data recording) the individual phases of the frequency-switched measurement, from eqns 1, 2, 4 and 5 we obtain;

$$\begin{aligned}[SIG/\Delta CAL^{SIG} - REF/\Delta CAL^{REF}](\nu) = \{&\Delta T_{rx}(\nu, \Delta\nu) + \Delta[T_{source} * g_{mb}](\nu, \Delta\nu) + \\ &\Delta[T_{2.7K} * g_{mb}](\nu, \Delta\nu) + \Delta T_{spill}(\nu, \Delta\nu)\} / T_{cal}\end{aligned} \tag{6}$$

where $\Delta x(\nu, \Delta\nu)$ is as defined above. Note that the variations with frequency introduced post-the calibration coupler have now been corrected for. Further, calibration into units of K can be obtained by multiplying the derived quantity by T_{cal}.

References

Briggs F.H., Sorar E., Kraan-Korteweg R.C., van Driel W., 1997, PASA, 14, 37
Emerson D.T., Klein U. & Haslam C.G.T., 1979, A&A, 76, 92
Liszt H., 1997, A&AS, 124, 183